

Research Article

Ionic Conductivity and Structural Evolution in $\text{Na}_2\text{B}_4\text{O}_7\text{--Bi}_2\text{O}_3$ Glasses: Influence of Bi_2O_3 Content and Temperature

Kuchakshoev Davlatnazar Sohibnazarovich ^{*}, **Dzhaborov Alexander Gulyamovich,**
Kholov Alimakhmad 

Umarov Sulton Umarovich Physical-Technical Institute, National Academy of Sciences of Tajikistan, Dushanbe, Tajikistan

Abstract

This study investigates the temperature-dependent electrical conductivity of glassy materials with compositions $\alpha \cdot \text{Bi}_2\text{O}_3 + (1-\alpha) \cdot \text{Na}_2\text{B}_4\text{O}_7$, where the Bi_2O_3 content varies from 10 to 30 mol.%. The motivation for this work arises from the growing interest in Bi_2O_3 -containing borate glasses as potential ionic conductors for electronic and photonic applications, as well as from the need to clarify the mechanisms governing charge transport in these systems. Electrical conductivity measurements were performed under controlled heating conditions with a constant heating rate, ensuring high reproducibility and reliability of the experimental data. The temperature dependence of conductivity was analyzed over a broad temperature range extending from ambient conditions up to approximately 680 K. In the low-temperature region (up to 420–450 K), only minor changes in conductivity were observed, indicating limited mobility of charge carriers and the dominance of localized transport processes. At higher temperatures, a pronounced increase in conductivity occurs, which is attributed to the thermally activated migration of mobile ions. The analysis of the conductivity data demonstrates that sodium ions act as the dominant charge carriers in the investigated compositions. This conclusion is supported by the characteristic Arrhenius-type behavior at elevated temperatures and by the absence of features typical for electronic conduction. Visual inspection of the samples after electrical measurements, complemented by scanning electron microscopy, confirms the preservation of the glassy state and supports the predominance of ionic conduction mechanisms. The results reveal a strong dependence of electrical conductivity on Bi_2O_3 concentration, reflecting composition-induced structural modifications of the glass network that influence ion mobility. Overall, the present study provides new insights into ion-transport mechanisms in $\text{Bi}_2\text{O}_3\text{--Na}_2\text{B}_4\text{O}_7$ glasses and highlights the critical role of glass composition in controlling their temperature-dependent electrical properties.

Keywords

Electrical Conductivity, Bi_2O_3 -containing Glass, $\text{Na}_2\text{B}_4\text{O}_7$, Ionic Transport, Temperature Dependence, Activation Energy

*Correspondence: Kuchakshoev Davlatnazar Sohibnazarovich (k.davlat@mail.ru)

Received: 3 January 2026; Accepted: 17 January 2026; Published: 2 June 2026



1. Introduction

Glasses containing bismuth oxide (Bi_2O_3) represent an important class of functional oxide materials due to their exceptional structural and physicochemical properties. The large polarizability of Bi^{3+} ions, combined with their low field strength, strongly affects the short- and medium-range order of the glass network and governs a wide range of thermal, optical, and transport characteristics. As a result, Bi_2O_3 -based glasses have found broad applications in photonic components, infrared optical systems, ionic conductors, and electronic devices, as well as in functional ceramics and glass-ceramics [1-5].

Bismuth oxide is particularly attractive for optical and electronic applications due to its high refractive index, low glass-transition and melting temperatures, and its ability to modify the connectivity of borate-based glass networks. Bi^{3+} can act not only as a network modifier but also as a network former through the formation of BiO_6 octahedral units, which contributes to the stabilization of the three-dimensional glass structure and significantly influences the glass properties [2]. The incorporation of Bi_2O_3 promotes the conversion of trigonal BO_3 units into tetrahedral BO_4 groups, leading to changes in boron coordination, network rigidity, and polarizability [6]. Such structural rearrangements directly influence ionic transport processes, which in oxide glasses are governed by composition, temperature, and the mobility of alkali ions acting as the primary charge carriers in the disordered network.

Electrical conductivity in glasses generally exceeds that of crystalline materials of comparable composition due to the absence of long-range periodicity and the presence of structural disorder, defects, and loosely bound oxygen configurations that facilitate ion mobility. Crystallization typically leads to a pronounced decrease in conductivity, as the formation of ordered phases and stronger chemical bonds restricts ionic transport and increases the activation energy [7]. Glasses generally exhibit higher conductivity than crystals due to the lack of long-range order and presence of structural defects that facilitate ion migration. Crystallization often reduces conductivity because ordered structures hinder ionic transport [8].

Existing studies indicate that multicomponent alkali-free or low-alkali bismuth borate glasses tend to exhibit predominantly ionic conduction, often characterized by unipolar transport mechanisms determined by a single type of mobile ion [9]. However, despite extensive research on binary Bi_2O_3 - B_2O_3 and Bi_2O_3 -modified borate systems, systematic investigations of electrical conductivity in Na-Bi-B oxide glasses remain scarce. In particular, for the system $(1-\alpha)\cdot\text{Na}_2\text{B}_4\text{O}_7 + \alpha\cdot\text{Bi}_2\text{O}_3$, the available data are largely limited to phase formation and glass stability. This system is thermodynamically unstable, and its state changes upon heating, which has been demonstrated experimentally [10-13]. For mixtures containing more than ~30 mol% Bi_2O_3 , multiphase crystalline compounds are typically reported, whereas lower Bi_2O_3 contents favor the formation of predominantly amorphous structures [14].

To the best of our knowledge, no comprehensive conductivity studies addressing the combined influence of Bi_2O_3 concentration and temperature on Na-containing bismuth borate glasses have been reported. This knowledge gap limits the understanding of ion transport mechanisms in Bi-rich borate networks and constrains the development of high-performance functional glasses for electronics and photonics.

The aim of the present work is therefore to investigate the temperature-dependent electrical conductivity of glasses in the system $\alpha\cdot\text{Bi}_2\text{O}_3 + (1-\alpha)\cdot\text{Na}_2\text{B}_4\text{O}_7$ across a wide range of compositions. The results obtained provide new insights into the role of Bi_2O_3 in modifying the structure and enhancing ionic transport in Na-Bi-B oxide glasses.

2. Experimental Methodology

2.1. Materials and Sample Preparation

Glass samples were prepared using sodium tetraborate ($\text{Na}_2\text{B}_4\text{O}_7 \cdot 10\text{H}_2\text{O}$, analytical grade) and bismuth oxide (Bi_2O_3 , high purity) as starting materials. To minimize crystallization water in $\text{Na}_2\text{B}_4\text{O}_7$ and remove adsorbed moisture from Bi_2O_3 , both components were preheated in a muffle furnace at 573 K for 2 hours in air.

For glass synthesis, the preheated sodium tetraborate was mixed with the calculated amount of Bi_2O_3 . Three compositions containing 10, 20, and 30 mol.% Bi_2O_3 were investigated, which, according to the literature, produce optically transparent glasses [15]. The resulting batch was ground in a ball mill for 1 hour to obtain a fine, homogeneous powder. The mixture was then melted in a platinum crucible at 1050 K with a holding time of 7 hours. After melting, the molten material was poured into a ceramic Al_2O_3 mold and cooled to room temperature. An ceramic crucible was employed as both the melting container and quenching mold due to the high reactivity of Bi_2O_3 -based melts with most materials at elevated temperatures.

The samples had a cylindrical geometry with diameters of 10–12 mm and thicknesses in the range of 2–10 mm [15]. The exact thickness L and electrode contact area S were measured individually for each sample and explicitly taken into account in the conductivity calculations.

Prior to measurements, both flat faces of each sample were mechanically polished to ensure parallelism and good electrical contact. Polished metallic silver electrodes with a diameter of 10 mm were used as current collectors. No silver paste or adhesive layers were applied, eliminating possible chemical interactions between the electrode material and the glass. The electrodes were pressed against the sample surfaces with a constant mechanical load to ensure reproducible contact conditions.

Electrical measurements were performed under a constant

applied DC voltage of 10 V. During heating, the electric current $I(T)$ flowing through the sample was continuously recorded as a function of temperature. The specific electrical conductivity σ was calculated using the standard relation for a homogeneous bulk sample:

$$\sigma = \frac{I \cdot L}{U \cdot S}$$

where U is the applied voltage, L is the sample thickness, and S is the electrode contact area.

Although AC impedance spectroscopy is widely used for separating bulk and interfacial contributions in ion-conducting materials, the DC method remains an established and informative approach for studying temperature-dependent ionic transport in alkali-containing oxide glasses, particularly at elevated temperatures where bulk ionic conduction dominates over electrode polarization effects [9, 16, 17]. In the present study, the use of DC voltage was deliberately chosen to enable direct observation of ion migration processes in Na^+ -containing glasses, including charge accumulation near the electrodes and irreversible redistribution effects occurring during thermal activation. Such effects are typically averaged out in AC impedance measurements but are clearly manifested under DC conditions, especially at elevated temperatures. In addition, the reproducibility of the electrical measurements was verified by performing repeated heating cycles on the same samples. Differences observed between the first and subsequent heating runs were reproducible and are attributed to thermally induced structural relaxation and redistribution of mobile Na^+ ions within the glass network rather than to experimental instability.

This DC methodology has been successfully applied in numerous studies of alkali-ion conducting borate and bismuth-

containing glasses and provides reliable information on activation energies and transport mechanisms when combined with careful control of experimental conditions [2, 3, 18].

According to our previously published study [10], the glass transition temperature of the investigated $\text{Na}_2\text{B}_4\text{O}_7\text{-Bi}_2\text{O}_3$ glasses lies in the range 710–770 K, depending on the Bi_2O_3 concentration. Since all electrical conductivity measurements were carried out up to 680 K, they were performed entirely below T_g , ensuring preservation of the amorphous glassy state during the experiments.

The amorphous nature of all prepared samples was confirmed by X-ray diffraction [19]. The XRD patterns exhibit a broad diffuse halo without any sharp diffraction peaks, indicating the absence of long-range crystalline order (Figure 1).

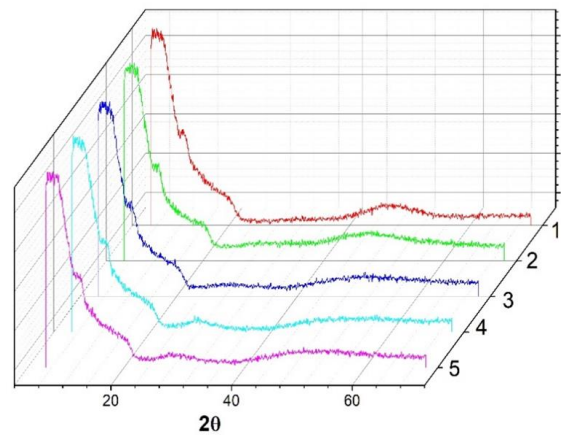


Figure 1. XRD patterns of $\text{Na}_2\text{B}_4\text{O}_7\text{-Bi}_2\text{O}_3$ glasses with different Bi_2O_3 contents. Sample 1 – 0 mol.% Bi_2O_3 ; Sample 2 – 10 mol.% Bi_2O_3 ; Sample 3 – 20 mol.% Bi_2O_3 ; Sample 4 – 30 mol.% Bi_2O_3 .

2.2. Electrical Conductivity Measurements

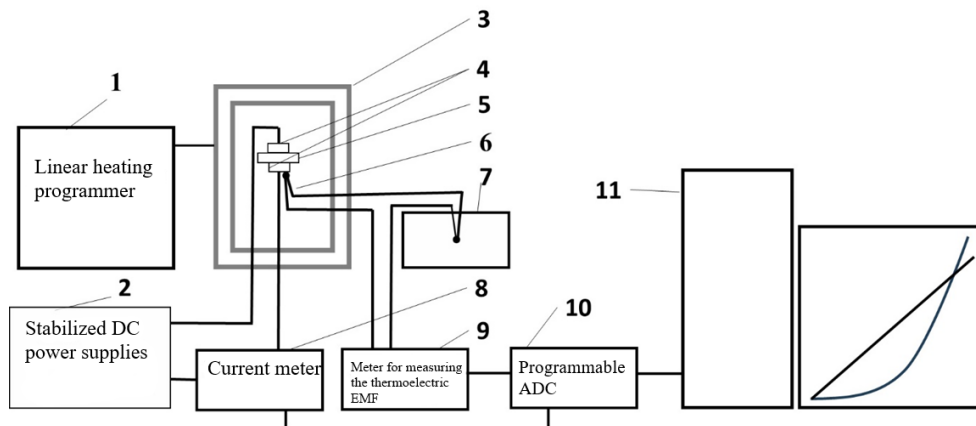


Figure 2. Experimental setup for high-temperature electrical measurements of solid materials: 1 – linear heating programmer; 2 – stabilized DC power supplies; 3 – furnace heater mounted on a lifting mechanism; 4 – silver electrodes; 5 – sample; 6 – differential thermocouple for measuring sample temperature; 7 – thermostated zero-junction block for the thermocouple; 8 – current meter; 9 – meter for measuring the thermoelectric EMF of the differential thermocouple; 10 – programmable ADC (Disco2); 11 – computer.

The temperature-dependent electrical conductivity was measured using a specially designed experimental setup, as shown schematically in Figure 2. The linear heating rate was controlled by a programmable controller (1), which regulated the voltage supplied to the furnace heater (3) mounted on a vertical stand. The polished glass sample (5) was placed between two silver electrodes (4) with a diameter of 8 mm. Temperature was monitored using a chromel–alumel (K-type) differential thermocouple (6), one end of which was attached to a zero-reference junction (7). A constant voltage was applied to the sample from a stabilized power supply (2). Conductivity current and thermoelectric voltage from the thermocouple were recorded using two microvolt–nanoammeters F-136 (8,

9). The analog signals were fed into a programmable ADC (10) and digitized via USB interface to a computer (11).

Data acquisition software displayed real-time graphs of current and thermoelectric voltage as functions of time and simultaneously saved the data in tabular text format for further processing in OriginLab.

2.3. Investigated Parameters

The study focused on the variation of electrical conductivity with temperature for the α : $\text{Bi}_2\text{O}_3 + (1-\alpha) \cdot \text{Na}_2\text{B}_4\text{O}_7$ system. Sample compositions, melting temperatures, and hold times are summarized in Table 1.

Table 1. Sample compositions, melting temperatures, and hold times.

Sample	Bi_2O_3 (mol.%)	$\text{Na}_2\text{B}_4\text{O}_7$ (mol.%)	Melting Temperature (K)	Hold Time (h)
1	0	100	1050	7
2	10	90	1050	7
3	20	80	1050	7
4*	30	70	1050	0
5	30	70	1050	7

*Sample 4 has the same composition as Sample 5, but was obtained without prolonged holding in the melt, whereas Sample 5 was produced with extended holding time.

3. Experimental Results

The temperature dependence of the specific electrical conductivity of α : $\text{Bi}_2\text{O}_3 + (1-\alpha) \cdot \text{Na}_2\text{B}_4\text{O}_7$ glasses, measured under a constant

heating rate, is presented in Figure 3. The conductivity curves can be conventionally divided into two regions: a low-temperature range (300–540 K) and a high-temperature range (540–680 K), allowing identification of several characteristic features in conductivity behavior.

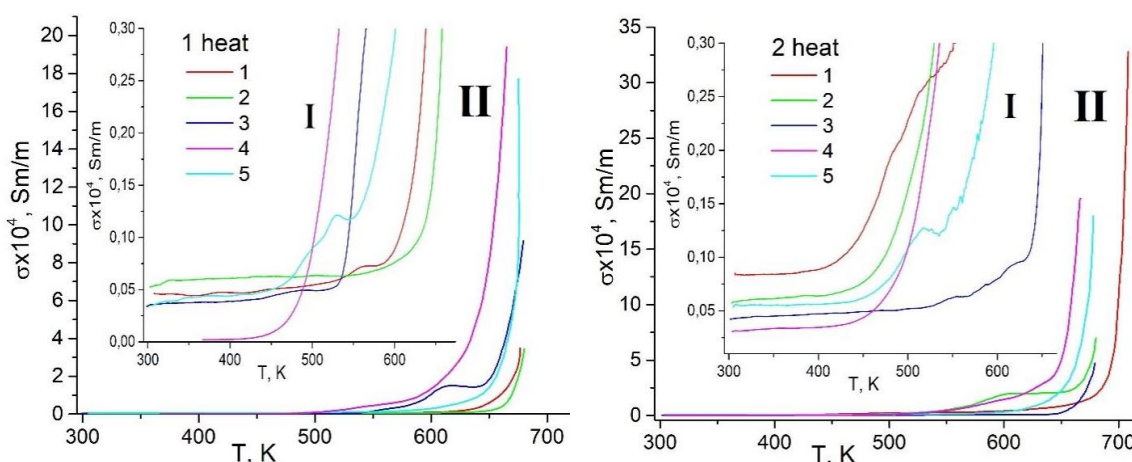


Figure 3. Temperature dependence of the specific electrical conductivity for α : $\text{Bi}_2\text{O}_3 + (1-\alpha) \cdot \text{Na}_2\text{B}_4\text{O}_7$ glasses with varying Bi_2O_3 content (10–30 mol.%) during the first heating cycle. Low-temperature (300–540 K) and high-temperature (540–680 K) regions are indicated. Sample numbering follows Table 1: Sample 1 – 0 mol.% Bi_2O_3 ; Sample 2 – 10 mol.% Bi_2O_3 ; Sample 3 – 20 mol.% Bi_2O_3 ; Sample 4 – 30 mol.% Bi_2O_3 .

In the low-temperature region, during the first heating cycle up to 420–450 K, all samples show minor changes in conductivity. This limited variation is attributed to the low concentration of mobile charge carriers, which are unable to move efficiently under the applied electric field at these temperatures. In this temperature range, Na^+ ions remain confined to deep potential wells formed by $\text{BO}_2\text{-BO}_4$ and Bi-O structural units. Charge transport is therefore limited to short-range hopping between neighboring sites without long-range diffusion, resulting in weak temperature dependence of conductivity. With increasing temperature, conductivity rises, exhibiting

maxima and inflection points, and above 480 K a sharp increase is observed. The rapid increase in conductivity above ~540 K coincides with the onset of intensive structural relaxation processes in the glass network, likely approaching the glass transition region. Thermal expansion and bond rearrangement reduce migration barriers for Na^+ ions, enabling long-range ionic transport. This behavior reflects an increase in the number of mobile charge carriers and the dominance of highly mobile ions at elevated temperatures. This process is more clearly illustrated by the concentration dependence of electrical conductivity (Figure 4).

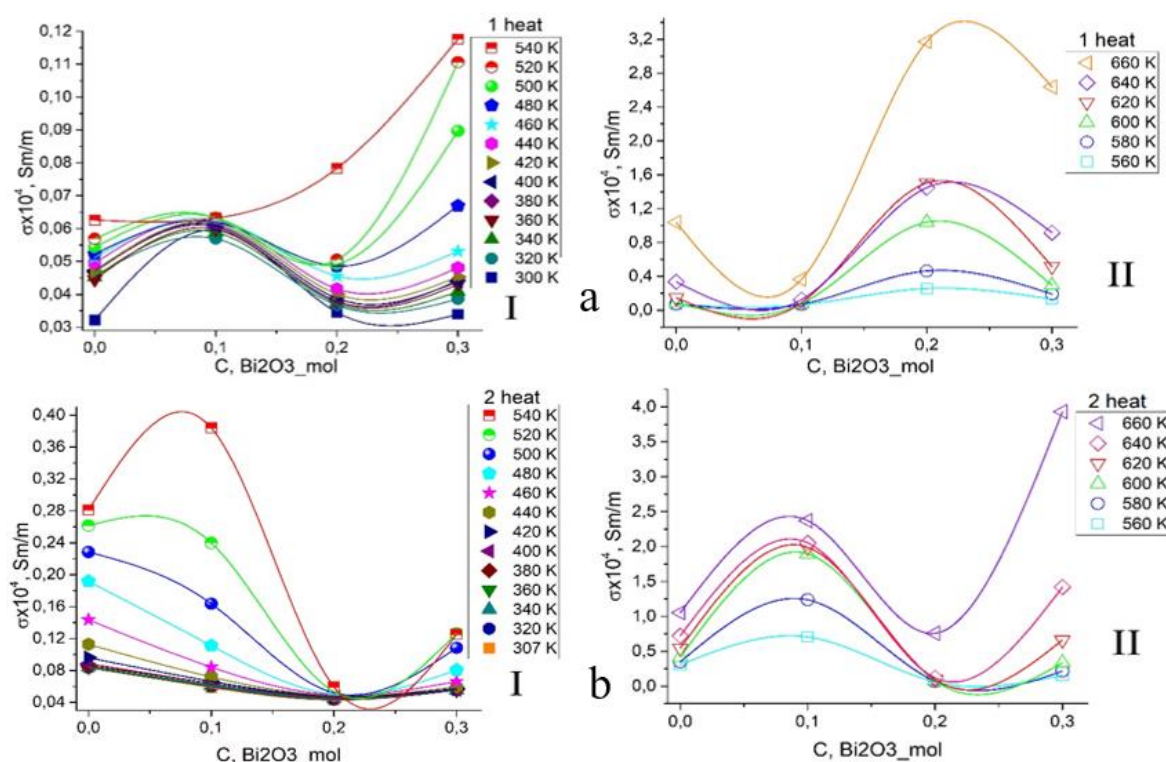


Figure 4. Effect of Bi_2O_3 concentration on electrical conductivity at (a) first heating and (b) second heating cycle. Low- and high-temperature trends illustrate compositional dependence of ionic transport.

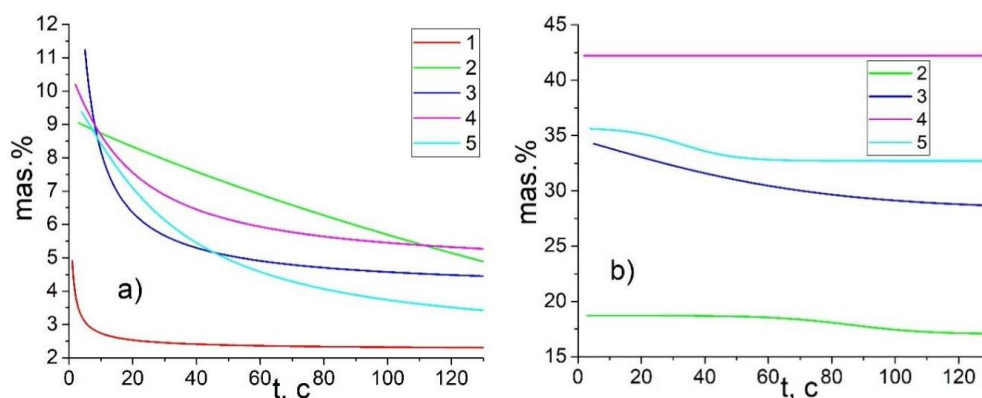


Figure 5. Time-dependent decay of Na^+ (a) and Bi (b) signals under electron beam exposure ($U = 20 \text{ kV}$, $I = 1 \text{ nA}$) observed via SEM-EDS, demonstrating high mobility of sodium ions relative to bismuth. Sample numbering follows Table 1: Sample 1 – 0 mol.% Bi_2O_3 ; Sample 2 – 10 mol.% Bi_2O_3 ; Sample 3 – 20 mol.% Bi_2O_3 ; Sample 4 – 30 mol.% Bi_2O_3 .

Evidence indicates that ionic conduction predominates in these glasses, with sodium ions serving as the primary charge carriers. Scanning electron microscopy (SEM) demonstrates that the signal intensity associated with sodium decreases exponentially over time under electron beam irradiation, whereas the signal from bismuth remains constant (Figure 5). Sodium ions can integrate into the network formed by BO_3 and BiO_3 units, forming ionic bonds with oxygen. High-field electron beam exposure ($U = 20 \text{ kV}$, $I = 1 \text{ nA}$) leads to the “washing-out” of sodium from the irradiated zone, highlighting its high mobility relative to other elements. This behavior

directly reflects the high mobility of Na^+ ions within the glass matrix and is consistent with their dominant role in field-driven ionic transport.

Visual observations after current passage and subsequent heating reveal black deposits on the cathode-facing surfaces of the samples (Figure 6), indicative of sodium accumulation. SEM analysis confirms increased sodium concentration in near-surface layers, which depends on the measurement duration (energy-dispersive spectrum acquisition time).

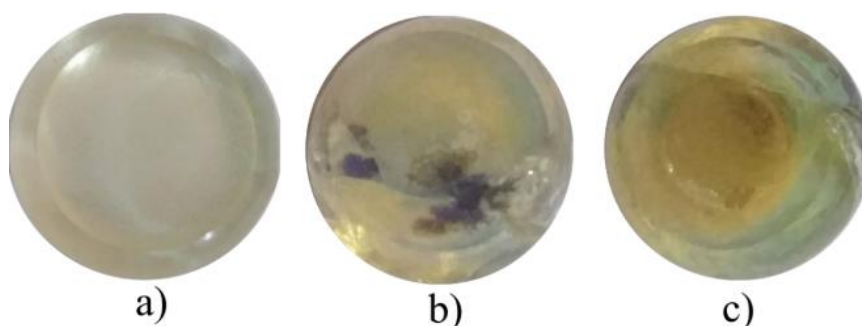


Figure 6. Photographs of glass samples after electrical current passage and heating: (a) general view, (b) black deposits on the cathode-facing surface indicative of sodium accumulation, (c) view of the sample from the anode side.

Figure 7 shows three points located in the light, gray, and black regions, while Figure 8 presents the corresponding elemental spectra. Elevated sodium concentrations are observed only in the black regions. In contrast, the anode-facing layer is characterized by reduced sodium content and the presence

of silver, which is attributed to interfacial diffusion from the Ag electrode at elevated temperatures. This diffusion is limited to the near-surface region and does not contribute to bulk electrical conduction, which is governed by the migration of Na^+ ions within the glass matrix.

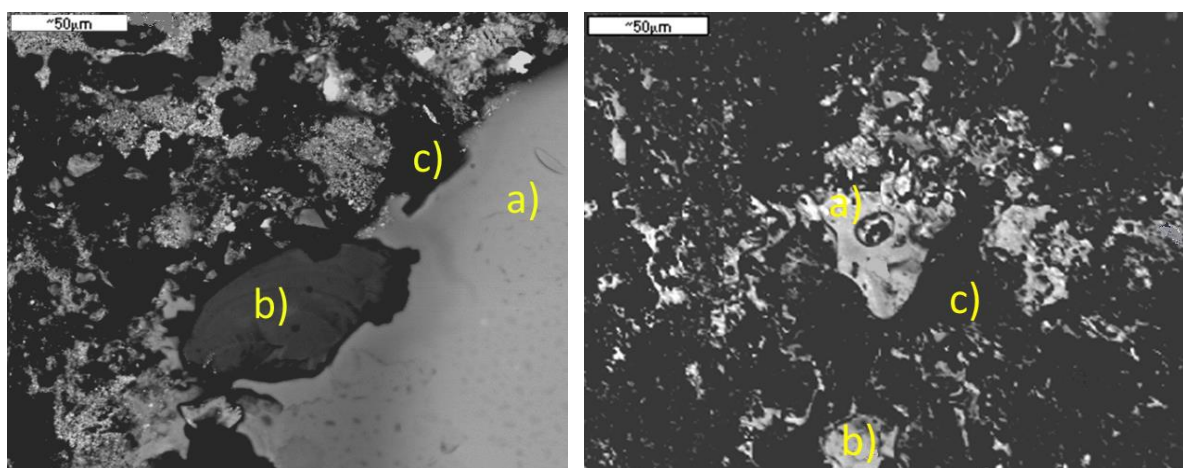


Figure 7. Selected surface regions for SEM-EDS analysis: (a) light, (b) gray, and (c) black areas. Locations correspond to spectra presented in Figure 8.

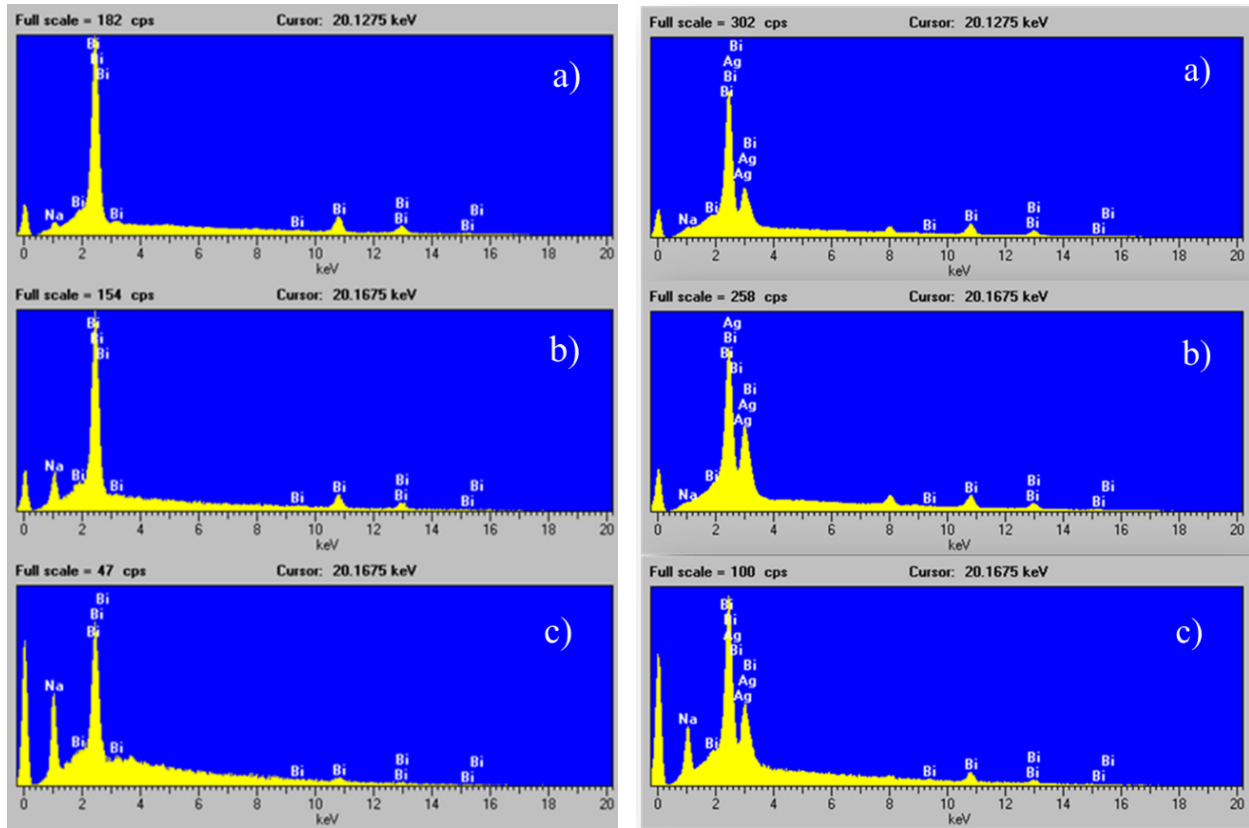


Figure 8. Elemental spectra from SEM-EDS analysis of selected surface regions shown in *Figure 7*. Increased Na concentration is observed in black regions, while the anode-facing layer shows reduced Na and presence of Ag due to electrode diffusion.

In the high-temperature region, the temperature dependence of electrical conductivity follows an Arrhenius-type behavior and can be described by

$$\sigma = \sigma_0 \exp\left(-\frac{W}{RT}\right), \quad (1)$$

where σ_0 is the pre-exponential factor, W is the activation energy of conductivity, R is the gas constant, and T is the absolute temperature. The activation energy W was determined from the slope of the linear regions in the $\ln\sigma$ versus $1/T$ plots (*Figure 9*) for each sample (*Table 2*).

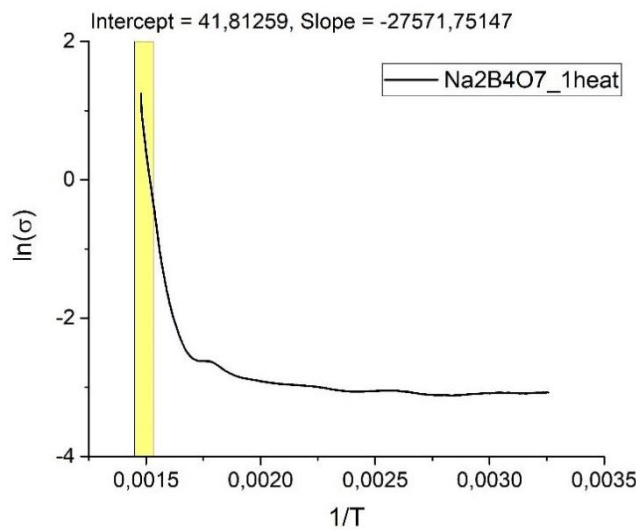


Figure 9. Arrhenius plot ($\ln\sigma$ vs. $1/T$) for one representative $\alpha\text{-Bi}_2\text{O}_3 + (1-\alpha)\text{-Na}_2\text{B}_4\text{O}_7$ glass sample. The linear region used for determination of activation energy W is indicated.

Figure 10 summarizes the activation energies for different Bi₂O₃ concentrations and for first and subsequent heating cycles. Significant differences are observed between heating cycles and temperature ranges, reflecting complex structural rearrangements.

The incorporation of Bi₂O₃ strongly affects the activation energy of conductivity. Observed variations are attributed to redistribution of structural units during preliminary heating,

resulting in altered local environments for sodium ions. Sodium delocalization at elevated temperatures, facilitated by lower activation energy relative to covalent bonds, enables ionic drift and charge transport. Cathode-side blackening further supports the role of Na⁺ as the primary charge carrier. The activation energy is not constant, indicating multi-stage conduction processes.

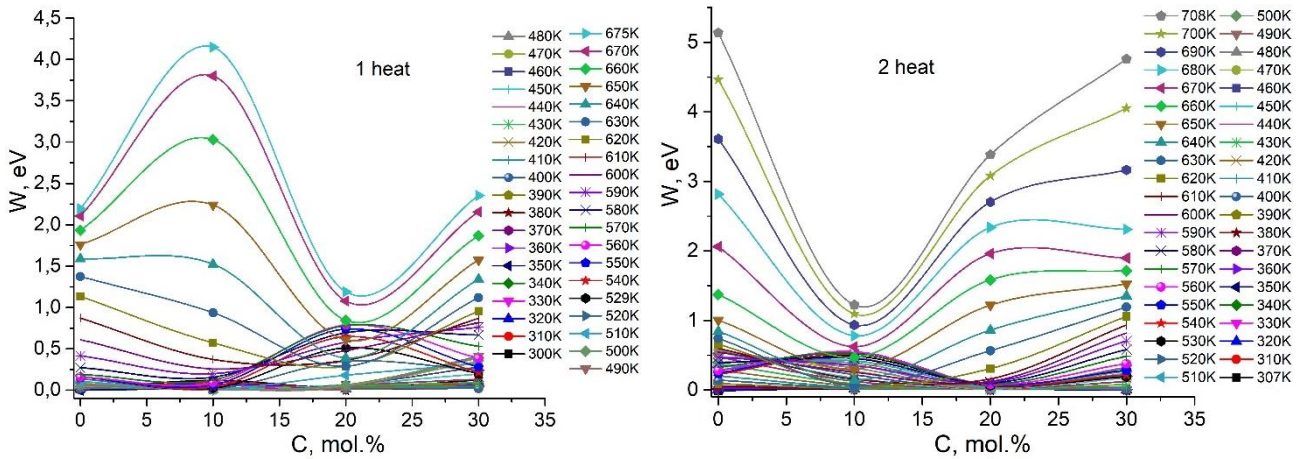


Figure 10. Activation energy of electrical conductivity as a function of Bi₂O₃ concentration for the first and second heating cycles.

The non-constant activation energy indicates the presence of multiple migration pathways for Na⁺ ions associated with different local structural environments. At lower temperatures, transport occurs via hopping between shallow sites near non-bridging oxygens, whereas at higher temperatures Na⁺ ions

overcome deeper potential barriers associated with more rigid borate–bismuth structural units. This results in a stepwise activation of conduction processes, manifested as multiple slopes in Arrhenius plots and differential conductivity maxima.

Table 2. Activation energy *W* (eV) of α -Bi₂O₃ + (1- α)-Na₂B₄O₇ glasses for different Bi₂O₃ concentrations during first and second heating cycles at high temperatures.

Sample	Bi ₂ O ₃ (mol.%)	W, 1st heating (eV)	W, 2nd heating (eV)
1	0	2.38	5.57
2	10	4.47	2.3
3	20	2.14	3.7
4	30	2.47	2.94
5	30	2.1	3.02

The contribution of ionic conductivity at low temperatures was estimated using the extrapolated $\ln \sigma_0$:

$$\sigma = \exp\left(\ln \sigma_0 - \frac{W}{RT}\right), \tag{2}$$

and by subtracting this value from the measured conductivity,

revealing differential conductance maxima associated with thermal activation of sodium ions from distinct bonding environments (Figure 11). These step-like features reflect multiple energy barriers encountered during ion migration. Integration of the conductivity curves yields the total transported charge *Q*, which varies among samples and heating cycles, reflecting structural

heterogeneity and redistribution of sodium-conducting pathways.

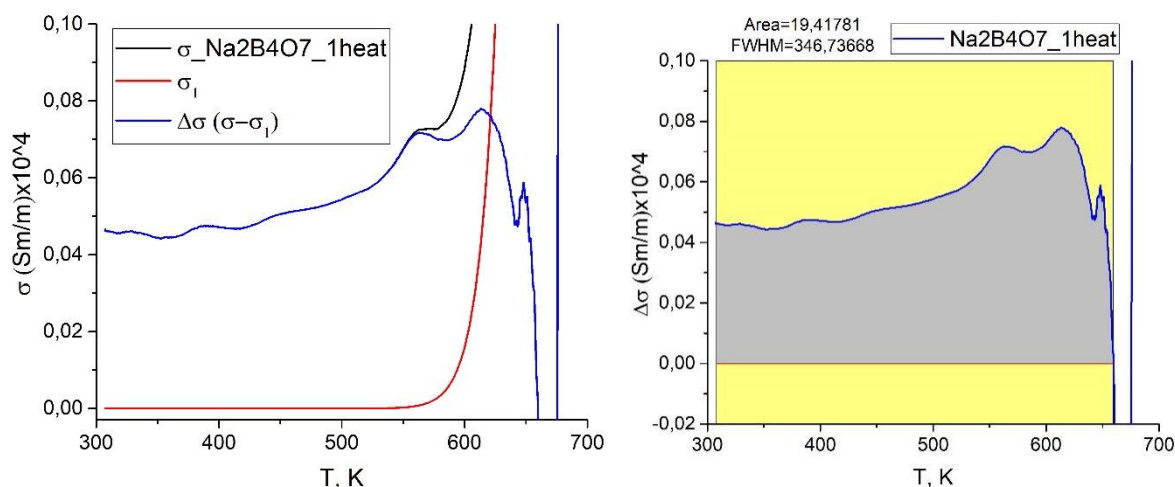


Figure 11. Example of processing experimental electrical conductivity data: on the left – curves obtained by subtracting calculated conductivity values (Equation (2)) from the experimentally measured $\sigma(T)$; on the right – the isolated contribution of ionic conductivity at low temperatures for the given sample.

The non-constant activation energy observed in different temperature ranges does not imply a change in the fundamental transport mechanism. Instead, it reflects the structural heterogeneity of the glassy network, where Na^+ ions occupy non-equivalent sites characterized by different local binding energies. As temperature increases, Na^+ ions are progressively activated from weaker to stronger binding environments, resulting in apparent variations of activation energy and step-like features in the differential conductivity curves.

4. Conclusions

No indications of electronic or mixed conductivity were found, and Na^+ ion transport remains the sole charge-transfer mechanism under the applied experimental conditions.

Although, in principle, electronic or mixed ionic–electronic conductivity could be considered in Bi-containing oxide glasses, no experimental evidence supporting such mechanisms is observed in the present study. The absence of mixed-valence Bi species, the high activation energies, and the strong correlation between conductivity behavior and Na redistribution indicate that charge transport is governed exclusively by Na^+ ionic migration within the investigated temperature range.

The ionic transport behavior of $\alpha\text{-Bi}_2\text{O}_3 + (1-\alpha)\text{-Na}_2\text{B}_4\text{O}_7$ glasses is governed by two temperature regimes: a nearly inert low-temperature region and a sharply increasing high-temperature region associated with the thermal activation of Na^+ ions. Repeated heating leads to noticeable restructuring of the glass network, resulting in opposite shifts of low- and high-temperature conductivity and reflecting partial recovery or redistribution of charge carriers. The influence of Bi_2O_3 is strongly

non-monotonic, indicating a complex interplay between composition and local structural environments. SEM–EDS results confirm that Na^+ ions dominate charge transport, consistent with cathode-side darkening and the decay of Na signals under electron-beam exposure. Arrhenius analysis shows that the activation energy of conductivity is not constant but varies with both composition and thermal history, indicating the presence of multiple energy barriers for Na^+ migration. The change in slope observed in $\ln\sigma$ versus $1/T$ plots occurs well below the glass transition temperature ($T_g = 710\text{--}770$ K, depending on Bi_2O_3 content) and therefore reflects a crossover between different ionic transport mechanisms rather than a glass transition or crystallization process. Differential conductivity analysis further supports a multistage, stepwise character of ion transport arising from Na^+ ions occupying structurally distinct environments.

Repeated heating cycles lead to partial redistribution of sodium ions and modification of the local glass structure, resulting in measurable differences in activation energy and conductivity behavior between the first and subsequent heating runs. The non-monotonic dependence of transport parameters on Bi_2O_3 concentration highlights the complex interplay between network connectivity, modifier-induced depolymerization, and ionic mobility.

Overall, this study clarifies the mechanisms governing Na^+ ion transport in Bi_2O_3 -containing borate glasses and demonstrates that compositional tuning and thermal treatment provide effective means for controlling ionic conductivity. These findings are relevant for the design of glassy materials for ion-conducting applications in electronic and electrochemical devices.

Abbreviations

SEM	Scanning Electron Microscopy
EDS	Energy Dispersive X-ray Spectroscopy

Author Contributions

Kuchakshoev Davlatnazar Sohbnazarovich: Data curation, Formal Analysis, Investigation, Writing – original draft

Dzhabarov Alexander Gulyamovich: Methodology, Software, Supervision, Validation, Writing – review & editing

Kholov Alimakhmad: Formal Analysis, Methodology, Supervision, Validation, Visualization, Writing – review & editing

Conflicts of Interest

The authors declare no conflict of interest.

References

- [1] Maeder T. (2013). Review of Bi₂O₃-based glasses for electronics and related applications. *International Materials Reviews*, 58(1), 3–40. <https://doi.org/10.1179/1743280412Y.0000000010>
- [2] Baia L., Stefan R., Kiefer W., Popp J., Simon S. (2002). Structural investigations of copper-doped B₂O₃–Bi₂O₃ glasses with high bismuth oxide content. *Journal of Non-Crystalline Solids*, 303(3), 379–386. [https://doi.org/10.1016/S0022-3093\(02\)01042-6](https://doi.org/10.1016/S0022-3093(02)01042-6)
- [3] Pan A., Ghosh A. (2002). Correlation of relaxation dynamics and conductivity spectra with cation constriction in ion-conducting glasses. *Physical Review B*, 66, 012301. <https://doi.org/10.1103/PhysRevB.66.012301>
- [4] Gomaa M. M., Ibrahim S., Darwish H. (2015). Effect of SiO₂/B₂O₃ replacements on the structure, physicochemical and electrical properties of Bi₂O₃-containing glasses. *Silicon*, 7(1), 55–63. <https://doi.org/10.1007/s12633-014-9213-3>
- [5] Dimitrov, V., & Sakka, S. (1996). Electronic oxide polarizability and optical basicity of simple oxides. *Journal of Applied Physics*, 79(3), 1736–1740. <https://doi.org/10.1063/1.360962>
- [6] El-Egili K., Ghazal R. (2021). Structural investigation of Fe₂O₃–Bi₂O₃–B₂O₃ glasses. *Egyptian Journal of Chemistry*, 64(8), 4069–4079. <https://doi.org/10.21608/ejchem.2021.67227.3454>
- [7] Silich, L. M. (1970). Change in electrical conductivity of glasses depending on heat treatment during the transition from the titanium-Celsius to the titanium-anorthite system. // In *Glass, Sitalts and Silicate Materials* (Issue 1. pp. 156-161). Minsk: Higher School. (in Russian).
- [8] Kuznetsov, A. Ya. (1959). Change in the electrical conductivity of glasses during crystallization. *Zhurnal Fizicheskoi Khimii*, 33, 1726–1732. (in Russian).
- [9] Mazurin, O. V. (1962). *Electrical Properties of Glass*. Leningrad: Goskhimizdat. (in Russian).
- [10] Kuchakshoev D. S., Dzhabarov A. G., Kholov A. (2023). Temperature dependence of the specific heat capacity of glasses based on Na₂B₄O₇ + Bi₂O₃. *Siberian Journal of Physics*, 18(3), 61–70. <https://doi.org/10.25205/2541-9447-2023-18-3-61-70>
- [11] D. S. Kuchakshoev, A. G. Dzhabarov, A. Kholov. (2023). Measuring the specific heat capacity of glass based on 2B₂O₃+Bi₂O₃ in a wide temperature interval. *Bulletin of the South Ural State University. Series: Mathematics. Mechanics. Physics*, 15(3), 89–96. (in Russian) <https://doi.org/10.14529/MMPH230310>
- [12] Kuchakshoev D. S. (2022). Effect of NaOH on the specific heat capacity of glasses of the B₂O₃–2Bi₂O₃ system depending on temperature. *Polytechnic Bulletin. Series: Intellect. Innovation. Investments*, 3(59), pp. 32–35. (in Russian).
- [13] Kuchakshoev D. S., Dzhabarov A. G., Kholov A. (2024). Temperature dependence of the specific heat of borate bismuth glasses with the addition of sodium. *Glass Physics and Chemistry*, 50(4), 390–397. <https://doi.org/10.1134/S1087659623600783>
- [14] Kuchakshoev, D., Dzhabarov, A. G. (2015). The differential thermal analysis of binary system Bi₂O₃ + Na₂B₄O₇. – *Doklady Akademii Nauk Respubliki Tajikistan*, v. 58, no. 11, pp. 1096-1099. (in Russian).
- [15] Kuchakshoev D. S., Dzhabarov A. G., Kholov A. (2020). Properties of glasses based on compounds Bi₂O₃ and Na₂B₄O₇. *Akad. Nauk Resp. Tadjh.*, 2020, vol. 63, nos. 7–8, pp. 488–493. (in Russian).
- [16] Jonscher, A. K. (1999). Dielectric relaxation in solids. *Journal of Physics D: Applied Physics*, v.32, Issue 14, pp. R57-R70. <https://doi.org/10.1088/0022-3727/32/14/201>
- [17] R. Long (1982). Frequency-dependent loss in amorphous semiconductors. *Advances in Physics*, 31(5), pp. 553–637. <https://doi.org/10.1080/00018738200101418>
- [18] M. D. Ingram (2006). Ionic conductivity and glass structure. *Philosophical Magazine B*, v.60, - Issue 6. pp. 729–740. <https://doi.org/10.1080/13642818908209739>
- [19] Kuchakshoev, D. S., Dzhabarov, A. G., Kholov, A. (2022). X-ray phase analysis of glasses (2Bi₂O₃–B₂O₃) and (Bi₂O₃–2B₂O₃) with different concentrations of NaOH in molding mixture. – *Dokl. Akad. Nauk Resp. Tadjh.*, vol. 65, nos. 1–2, pp. 69–74.